Biotechnol Lett (2020) 42:537–549
https://doi.org/10.1007/s10529-020-02802-7

ORIGINAL RESEARCH PAPER

# Disruption of the lactate dehydrogenase and acetate kinase genes in *Klebsiella pneumoniae* HD79 to enhance 2,3-butanediol production, and related transcriptomics analysis

**Jingping Ge · Jiawang Wang · Guangbin Ye · Shanshan Sun · Rui Guo · Gang Song · Wenxiang Ping**

Received: 26 August 2019 / Accepted: 13 January 2020 / Published online: 23 January 2020


**Abstract**
*Objectives* 2,3-Butanediol (2,3-BD) is widely used in several chemical syntheses as well as the manufacture of plastics, solvents, and antifreeze formulations, and can be manufactured by microbial glucose fermentation. Conventional (2,3-BD) fermentation typically has low productivity, yield, and purity, and is expensive for commercial applications. We aimed to delete the lactate dehydrogenase and acetate kinase (*ldh*A and *ack*) genes in *Klebsiella pneumoniae* HD79 by using λRed homologous recombination technology, to eliminate by-products and thereby improve (2,3-BD) production. We also analyzed the resulting gene changes by using transcriptomics.
*Results* The yield of (2,3-BD) from the mutant *Klebsiella* strain was 46.21 g/L, the conversion rate was 0.47 g/g, and the productivity was 0.64 g/L·h, which represented increases of 54.9%, 20.5%, and 106.5% respectively, compared to (WT) strains. Lactate and acetate decreased by 48.2% and 62.8%, respectively. Transcriptomics analysis showed that 4628 genes were differentially expressed (404 significantly up-regulated and 162 significantly down-regulated). Moreover, the (2,3-BD) operon genes were differentially expressed.
*Conclusion* Our data showed that the biosynthesis of (2,3-BD) was regulated by inducers (lactate and acetate), a regulator (*Bud*R), and carbon flux. Elimination of acidic by-products by *ldh*A and *ack* knockdown significantly improved (2,3-BD) production. Our results provide a deeper understanding of the mechanisms underlying (2,3-BD) production, and form a molecular basis for the improvement this process by genetic modification in the future.

**Keywords** *Klebsiella pneumoniae* · Lactate dehydrogenase · Acetate kinase · 2,3-Butanediol · Transcriptomics

J. Ge · J. Wang · G. Ye · S. Sun · R. Guo · G. Song · W. Ping (✉)
Engineering Research Center of Agricultural Microbiology Technology, Ministry of Education, Heilongjiang University, Harbin 150500, China
e-mail: wenxiangp@aliyun.com

J. Ge · J. Wang · G. Ye · S. Sun · R. Guo · G. Song · W. Ping
Key Laboratory of Microbiology, College of Heilongjiang Province, School of Life Sciences, Heilongjiang University, Harbin 150080, China

G. Ye
Youjiang Medical University for Nationalities, Baise 533000, China

## Introduction

2,3-Butanediol (2,3-BD) is widely used in many chemical syntheses (Białkowska 2016; Harvianto et al. 2018), as well as in the production of plastics,

solvents, and antifreeze formulations (Taeyeon et al. 2016). Increasing attention to environmental problems and fossil fuel resources have resulted in a growing interest in the production of 2,3-BD by microbial fermentation. However, conventional 2,3-BD fermentation processes show low productivity, yield, and purity, and are expensive for commercial applications (Yang and Zhang 2018).

Several microorganisms such as *Bacillus*, *Enterobacter*, *Serratia*, *Paenibacillus*, *Klebsiella*, *Saccharomyces cerevisiae*, and *Escherichia coli* produce relatively large amounts of 2,3-BD (Gao et al. 2018; Ishii et al. 2018). *Bacillus subtilis*, *B. licheniformis*, and *B. amyloliquefaciens* exhibit good 2,3-BD production (Ge et al. 2016; Sikora et al. 2015). However, *Klebsiella* strains appear to be the most suited to fermentative 2,3-BD production. In fed-batch glycerol fermentation with *K. pneumoniae*, the yield of 2,3-BD was 49.2 g/L (Petrov and Petrova 2009). Park et al. (2015) reported that *K. oxytoca* (Δ*ldh*A *Δpfl*B *ΔBud*C::PBDH) with intermittent glucose feeding showed a (R, R)-2,3-BD production of 106.7 g/L. Rathnasingh et al. (2016) deleted genes associated with lactate, ethanol, and acetate formation in *K. pneumoniae*, which resulted in higher titers and yields of 2,3-BD. *K. pneumoniae* HD79 produces 2,3-BD by a typical production machinery.

Glucose is used as a substrate in microbial fermentation for the synthesis of several proteins, nucleic acids, and other substances required for cell growth. Microbial fermentation of glucose is usually accompanied by the formation of various metabolites and by-products (Yang et al. 2017). The typical synthetic route for microbial 2,3-BD production is conversion of polysaccharide to pyruvate, α-acetolactate, acetoin, and ultimately 2,3-BD. This process produces ethanol, acetate, lactate, succinate, 1,3-propanediol (1,3-PD), and other by-products, which consume energy, and are not conducive to 2,3-BD (Park et al. 2016) production. Thus, 2,3-BD production could be improved by eliminating or controlling the production of metabolic by-products.

In this work, λRed homologous recombination technology was used to knock out the lactate dehydrogenase and acetate kinase genes *ldh*A and *ack* from *K. pneumoniae* HD79, in order to eliminate lactate and acetate formation, and thereby increase 2,3-BD production. We then studied the effects of *ldh* and *ack* on the production of 2,3-BD from glucose fermentation by comparing the transcriptomic profiles of the knockout and wild-type (WT) strains, and identified significantly up- and down-regulated genes.

## Materials and methods

### Bacterial strains and growth conditions

All strains and plasmids used or created in this work, along with their sources and characteristics are shown in Table 1. *E. coli* DH5α was grown in Luria–Bertani (LB) medium (1% tryptone, 0.5% yeast extract, and 1% NaCl; w/v). *K. pneumoniae* HD79, designated the WT strain, was grown at 30 °C in medium containing 150 g/L glucose, 5 g yeast extract, 0.05 g $FeSO_4{\cdot}7H_2O$, 0.001 g $ZnSO_4{\cdot}7H_2O$, 0.001 g $MnSO_4{\cdot}H_2O$, 0.001 g $CaCl_2{\cdot}2H_2O$, 0.25 g $MgSO_4{\cdot}7H_2O$, 6.6 g $(NH_4)_2SO_4$, 8.7 g $K_2HPO_4$, and 6.8 g $KH_2PO_4$ in 1 L $H_2O$. The initial pH was adjusted to 7.0 by adding 5 M KOH. The loading volume was 125 mL/250 mL. Flask cultures were maintained at 150 rpm for 12 h. *K. pneumoniae* HD79-01 was grown with 150 μg/mL chloramphenicol in the aforementioned medium. *K. pneumoniae* HD79-02 was grown with 150 μg/mL chloramphenicol and 125 μg/mL kanamycin in the same medium.

### Generation of *ldh* and *ack* knockout mutants

The *ldh*A (GenBank accession number JX104342.1) of *K. pneumoniae* HD79 was amplified by polymerase chain reaction (PCR) by using the following primers: *ldh*AL-forward (5′-GGAAGATCTCAGTACGACAAGAAGTATCTG-3′, *Bgl*II), *ldh*AL-reverse (5′-CCGCTCGAGACCGAAGCCTTTAAGAATGCGCAGC-3′, XhoI); *ldh*AR-forward (5′-CCGCTCGAGCTTCGGTATGCGCCTGCT-3′, XhoI), and *ldh*AR-reverse (5′-GGAGGATCCTCAGACCAGCGCGTTAGGG-3′, *Bam*HI). To clone $Cm^r$, pGP704-Cm was used as a template with the following primers: $Cm^r$-forward (5′-CCGCTCGAGGCTTGCGCAGACCAAAACG-3′, XhoI) and $Cm^r$-reverse (5′-CCGCTCGAGGCAGGCATGCAAGCTTGGT-3′, XhoI). The *ldh*A-L and *ldh*A-R genes were cloned into pMD18-T (TaKaRa, Dalian, China) to construct p*ldh*A-L and p*ldh*A-R, respectively. The $Cm^r$ was ligated into pMD18-T to construct pT-$Cm^r$. Disrupted *ldh*A was constructed by inserting a $Cm^r$ cassette into

**Table 1** Strains and plasmids used in this study

| Strain or plasmid | Characteristics | Source/reference |
|---|---|---|
| *E. coli* DH5α | $Ap^r$ | Laboratory preservation |
| *K. pneumoniae* HD79 | Wild-type | Laboratory preservation |
| *K. pneumoniae* HD79-01 | Δ*ldh*A, $Cm^r$ | Mutant from gene disruption; this study |
| *K.pneumoniae* HD79-02 | Δ*ldh*A, Δ*ack*, $Kan^r$, $Cm^r$ | Mutant from gene disruption; this study |
| pGP704-Cm | $Cm^r$ | Laboratory preservation |
| pKD46 | Exo, Bet, Gam, $Ap^r$ | Laboratory preservation |
| pMD18-T | Cloning vector $Ap^r$ | Takara Biotechnology Co. Ltd |
| p*ldh*A-L | *ldh*A-L, $Ap^r$ | Insertion of *ldh*A-L into pMD18-T; this study |
| p*ldh*A-R | *ldh*A-R, $Ap^r$ | Insertion of *ldh*A-R into pMD18-T; this study |
| p*ldh*A-LR | *ldh*A-LR, $Ap^r$ | Insertion of *ldh*A-LR into pMD18-T; this study |
| pT-*Cmr* | $Cm^r$, $Ap^r$ | Insertion of $Cm^r$ into pMD18-T; this study |
| pT-LCR | *ldh*AL-$Cm^r$-*ldh*AR, $Cm^r$, $Ap^r$ | Insertion of $Cm^r$ into p*ldh*A-LR; this study |
| pET-28a( +) | $Kan^r$ | Laboratory preservation |
| p*ack*-L | *ack*-L, $Ap^r$ | Insertion of *ack*-L into pMD18-T; this study |
| p*ack*-R | *ack*-R, $Ap^r$ | Insertion of *ack*-R into pMD18-T; this study |
| p*ack*-LR | *ack*-LR, $Ap^r$ | Insertion of *ack*-LR into pMD18-T; this study |
| pT-$Kan^r$ | $Kan^r$, $Ap^r$ | Insertion of $Kan^r$ into pMD18-T; this study |
| pT-LKR | *ack*L-$Kan^r$-*ack*R, $Kan^r$, $Ap^r$ | Insertion of $Kan^r$ into p*ack*-LR; this study |

the middle of *ldh*A obtained from *K. pneumoniae* HD79. The p*ldh*A-LR was constructed by inserting the XhoI–EcoRI fragment containing *ldh*A-R into the XhoI–EcoRI sites of p*ldh*A-L. After using restriction enzyme XhoI to digest pT-$Cm^r$ and p*ldh*A-LR, the $Cm^r$ fragment was inserted into the XhoI site of p*ldh*A-LR. Finally, pT-LCR containing interrupted *ldh*A (i.e. *ldh*AL-$Cm^r$-*ldh*AR) was linearized with restriction enzymes *Bgl*II and *Bam*HI. The fragment *ldh*AL-$Cm^r$-*ldh*AR was used in the λRed replacement approach to transform *K. pneumoniae* HD79 and obtain *K. pneumoniae* HD79-01.

The *ack* (GenBank accession number CP003218.1) of *K. pneumoniae* HD79-01 was amplified by PCR with the following primers: *ack*L-forward (5′-GGAAGATCTTGAACTGCGGTAGCTCCTCTCTGAA-3′, *Bgl*II), *ack*L-reverse (5′-CCGCTCGAGCTGAATTACGGACTCGTCGATCACC-3′, XhoI); *ack*R-forward (5′-CCGCTCGAGCAGACCATGCCGGAAGAATCCTATC-3′, XhoI), and *ack*R-reverse (5′-CGCGGATCCGGTGTCGTGCAGATGGAAGATGATG-3′, *Bam*HI). To clone $Kan^r$, pET-28a(+) was used as a template with the following primers: $Kan^r$-forward (5′-CCGCTCGAGTACATAAACAGTAATACAAGGGGTG-3′, XhoI) and $Kan^r$-reverse (5′-CCGCTCGAGATTAATTCTTAGAAAAACTCATCGA-3′, XhoI). The *ack*-L and *ack*-R were cloned into pMD18-T to construct p*ack*-L and p*ack*-R, respectively. The $Kan^r$ was ligated into pMD18-T to construct pT-$Kan^r$. Disrupted *ack* was constructed by inserting the $Kan^r$ cassette into the middle of *ack* obtained from *K. pneumoniae* HD79-01. The p*ack*-LR was constructed by inserting a XhoI-*Hin*dI fragment containing *ack*-R into the XhoI-*Hin*dI sites of p*ack*-L. After using the restriction enzyme XhoI to digest pT-$Kan^r$ and p*ack*-LR, the $Kan^r$ was inserted into the XhoI site of p*ack*-LR. Finally, pT-LKR containing the interrupted *ack* (i.e. *ack*L–$Kan^r$–*ack*R) was linearized with restriction enzymes *Bgl*II and *Bam*HI. The fragment *ack*L–$Kan^r$–*ack*R was used in the same approach to transform *K. pneumoniae* HD79-01 to obtain the *K. pneumoniae* HD79-02.

## Transformation by electroporation

We then introduced linear target fragment *ldh*AL–$Cm^r$–*ldh*AR into the genome of *K. pneumoniae* HD79 by homologous recombination. First, the plasmid pKD46 was transformed into *K. pneumoniae* HD79; cells were cultured in medium containing 5 mM L-

arabinose, inducing expression of Exo, Bet, and Gam. The linear target fragment *ldh*AL–*Cm*$^r$–*ldh*AR was then transformed into *K. pneumoniae* HD79, which was plated on agar containing 150 μg/mL chloramphenicol. Finally, the target fragment *ldh*AL–*Cm*$^r$–*ldh*AR was amplified by PCR.

The same approach was used to introduce the target fragment *ack*L–*Kan*$^r$–*ack*R into the genome of *K. pneumoniae* HD79-01, which was plated on agar containing 150 μg/mL chloramphenicol and 125 μg/mL kanamycin. The target fragment *ack*L–*Kan*$^r$–*ack*R was amplified by PCR.

## Real-time quantitative polymerase chain reaction to measure *ldh* and *ack*

RNA was extracted from *K. pneumoniae* HD79 and *K. pneumoniae* HD79-02 by using the RNA Prep Pure Bacteria Kit (Tiangen Biotech Co. Ltd., China). Reverse transcription was performed using the BioRT cDNA First Strand Synthesis Kit (Bioer Technology Co. Ltd., China; Mayer et al. 1995). Real-time Quantitative Polymerase Chain Reaction (qRT-PCR) was performed with at least three biological replicates using SYBR Green-based detection in triplicate in a 7500 Real-Time PCR System (Applied Biosystems, Inc., USA). The 16S rRNA gene was chosen as an internal control to normalize RNA amounts. The following primers were used: *ldh* (forward 5′-CCGC TCGAGCTTCGGTATGCGCCTGCT-3′, reverse 5′-GGAGGATCCTCAGACCAGCGCGTTAGGG-3′); *ack* (forward 5′-CCGCTCGAGCAGACCATGCCGGAA GAATCCTATC-3′, reverse 5′-CGCGGATCCGGT GTCGTGCAGATGGAAGATGATG-3′); 16S rRNA (forward 5′-AGAAGAAGCACCGGCTAACTC-3′, reverse 5′-CTCTACGCATTTCACCGCTAC-3′). Diluted cDNA equivalent to 1 ng RNA starting material was used as the template for qRT-PCR amplification. The transcriptional levels of *ldh* and *ack* were normalized to the transcriptional level of the 16S rRNA gene. The relative changes (*x*-fold) at the transcriptional level in different samples were calculated.

## SDS-PAGE

SDS-PAGE was performed using the protocol of Bio-Rad Laboratories, Inc. (Hercules, CA, USA). Protein samples were subjected to electrophoresis (JY-SCZ2+ , Beijing JUNYI Electrophoresis Co. Ltd., Beijing, China) at a constant 140 V until the tracking dye reached the bottom of the gel. The gels were stained with Coomassie Brilliant Blue for 15 min and destained with a solution containing 20% methanol and 10% acetic acid. Finally, the target protein bands were viewed and the gray value (the quantified color of target protein band) was analyzed by AlphaImager HP gel imaging system (AlphaImager HP, Protein Simple, USA).

## Enzyme assays

The precipitate from 6 mL fermentation broth was centrifuged at 5000 rpm for 10 min at 4 °C, washed twice with potassium phosphate buffer (100 mM, pH 7.4), and resuspended in the same buffer. The supernatant from broken cells was obtained by ultrasonic treatment in an ice-water bath and subsequent centrifugation (10,000 rpm, 10 min, and 4 °C), and used as crude liquor for the measurement of enzyme activities. An enzyme unit is defined as the amount of enzyme required to consume 1 μmol of substrate per minute.

## Fermentation kinetics

Batch fermentation was performed in 500 mL flasks containing 150 mL fermentation medium with an initial pH 6.8, with glucose as the substrate. Flasks were cultured at 30 °C with shaking at 150 rpm for 156 h. Samples were harvested every 12 h and transcriptome analysis was performed at 6 h. The sample was diluted tenfold and the optical density (OD) measured at 600 nm was used to describe cell growth. The concentrations of glucose, 1,3-PD, 2,3-BD, ethanol, acetate, succinate, and lactate obtained from the batch fermentation process were determined using a High Performance Liquid Chromatography (HPLC) system (Shimadzu Corp. Kyoto, Japan). The sample was diluted 100-fold, and an Aminex HPX-87H column (Bio-Rad Laboratories) was used with 0.005 M $H_2SO_4$ as the elution solvent at a flow rate of 0.8 mL/min, with the column oven temperature maintained at 65 °C with a refractive index detector.

## Library preparation

Total RNA was treated with DNase I prior to library construction, and poly-(A) mRNA and double-

stranded cDNA were purified using AMPure XP beads. Double-stranded cDNA was further subjected to end-repair with A tailing and ligated to the U-adaptor by using T4 DNA polymerase, Klenow fragment, and T4 polynucleotide kinase, followed by single dNTP base addition using the 3′ to 5′ exo-polymerase activity of Klenow fragment, and ligation to an adapter or index adapter using T4 DNA ligase. Adaptor-ligated fragments were separated on 1% agarose gel, and cDNA fragments of the desired size were excised. The first chain cDNA containing U was degraded using the USER enzyme, and PCR was performed to selectively enrich and amplify cDNA fragments. After validation with an Agilent 2100 Bioanalyzer and ABI StepOnePlus Real-Time PCR System, the cDNA library was subjected to Solexa sequencing using an Illumina HiSeq2000 sequencing platform.

### De novo assembly and annotation

Illumina HiSeq 2000/MiSeq was performed to generate sequencing reads, and the NGS QC Toolkit (https://59.163.192.90:8080/ngsqctoolkit/) was used to analyze raw count data, which was compared with the reference genome and reference genes using Bowtie2 (https://bowtie-bio.sf.net/bowtie2; Theissinger et al. 2016). Sequences were annotated using sequential BLAST searches designed to identify the most descriptive annotation for each sequence. Assembled unique transcripts were compared with sequences using the BLAST algorithm, and GO accessions of the highest hits were retrieved and mapped to GO terms according to molecular function, biological process, and cellular component ontologies (https://www.geneontology.org/; Harney et al. 2016). Remaining sequences encoding putative proteins were searched against the SwissProt (https://www.expasy.ch/sprot), KEGG, and COG (https://www.ncbi.nlm.nih.gov/COG) databases, with a typical E-value threshold of less than $10^{-5}$ (Kanehisa et al. 2017). Samples from different compartments were analyzed with EdgeR (https://www.bioconductor.org/packages/release/bioc/html/edgeR.html) to determinate the statistical significance of differential expression (Dimont et al. 2015).

### Validation of differentially expressed genes by qRT-PCR

qRT-PCR was performed to exclude false positives from high-throughput mRNA sequencing (RNA-seq). Four differentially expressed genes involved in 2,3-BD biosynthesis were chosen; the primers up (5′-GGATCCATGGAACTTCGTTATCTTCGCT-3′) and down (5′-GTCGACTCAGAACATCGCCA-GAAACG-3′) were used for amplification.

### Statistical analysis

Each experiment was repeated independently three times. JMP 10.0 software was used for statistical analyses. One-way analysis of variance (ANOVA) was used to analyze the differences between the experimental data. $P < 0.05$ (represented by *) was considered a significant difference; $P < 0.01$ (represented by **) was considered an extremely significant difference. Sigmaplot 12.5 software was used for statistical data analysis and chart analysis.

## Results

### Assay of *ldh* and *ack* knockout mutants

Characterization of the *ldh*A and *ack* knockout mutants is shown in Fig. 1. We observed a clear band of 1765 bp (*ldh*AL–*Cm*$^r$–*ldh*AR), which likely represents homologous recombination of the fragment into the chromosome of *K. pneumoniae* HD79 (Fig. 1a), and a clear band about 876 bp (*Cm*$^r$), which was absent in the control strain (Fig. 1b). The mutant strain *K. pneumoniae* HD79-01 was therefore obtained by integration of the *Cm*$^r$ cassette into the genome of *K. pneumoniae* HD79.

As shown in Fig. 1c, we observed a clear band of about 1433 bp (*ack*L-*Kan*$^r$-*ack*R), which indicates homologous recombination of this fragment into the chromosome of *K. pneumoniae* HD79-01. We also observed a clear band of about 813 bp (*Kan*$^r$), which was not seen in the control strain (Fig. 1d). The mutant strain *K. pneumoniae* HD79-02 was obtained therefore by integration of the *Kan*$^r$ cassette into the genome of *K. pneumoniae* HD79-01.

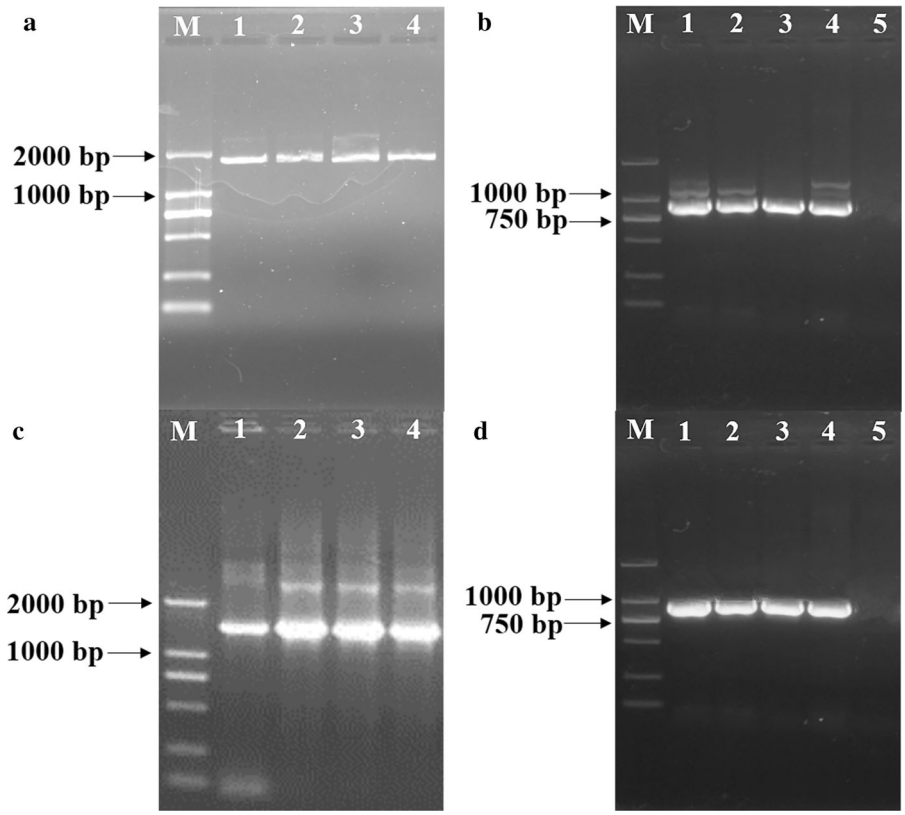


**Fig. 1** Amplification of *ldh*A and $Cm^r$ (**a**, **b**) and *ack* and $Kan^r$ (**c**, **d**). M is the marker of 2000; **a** Lanes 1–4 represent the genome of *K. pneumoniae* HD79-01 as template. **b** Lanes 1–4 represent the genome of *K. pneumoniae* HD79-01 as the template, Lane 5 represents the genome of *K. pneumoniae* HD79 as the template. **c** Lanes 1–4 represent the genome of *K. pneumoniae* HD79-02 as the template. **d** Lanes 1–4 show the genome of *K. pneumoniae* HD79-02 as the template, and lane 5 represents the genome of *K. pneumoniae* HD79-01 as the template

## Expression of *ldh* and *ack* mRNA

There was a significant reduction in *ldh* mRNA expression in *K. pneumoniae* HD79-02 compared to that in *K. pneumoniae* HD79. The transcription levels at 24 h, 48 h, and 72 h decreased by 76%, 74%, and 66% respectively, indicating successful disruption of *ldh* expression. There was also a significant reduction in *ack* mRNA levels in *K. pneumoniae* HD79-02 compared to those in *K. pneumoniae* HD79. The transcription levels at 24 h, 48 h, and 72 h decreased by 95.3%, 79.2%, and 76% respectively, indicating successful disruption of *ack* expression.

## Protein expression

The protein expression pattern in *K. pneumoniae* HD79-02 was studied. Expression of LDH and ACK were analyzed by grayscale values using a gel imaging system. LDH and ACK levels decreased by 72.2% and 59% respectively compared with those in *K. pneumoniae* HD79 ($P < 0.05$). Thus, the disruption of *ldh*A and *ack* in the recombinant strain *K. pneumoniae* HD79-02 successfully reduced the expression of LDH and ACK.

## Enzyme assays

The LDH and ACK activity in *K. pneumoniae* HD79-02 were reduced by 55.9% and 73.4% respectively compared with that in *K. pneumoniae* HD79. Thus, the disruption of *ldh* and *ack* in the recombinant strain *K. pneumoniae* HD79-02 successfully reduced enzyme activity.

## Fermentation kinetics analysis

The batch fermentation kinetics of *K. pneumoniae* HD79 and *K. pneumoniae* HD79-02 are shown in Fig. 2a. The growth of the WT strain was superior to that of the recombinant strain. The rate of glucose consumption was also significantly higher in the parental strain (Fig. 2b). The concentration of 2,3-BD produced by the mutant strains reached a maximum of 46.21 g/L at 72 h, whereas 2,3-BD concentration for the WT strain was 29.83 g/L (96 h); the 2,3-BD concentration for the recombinant strain was 1.55 times greater than that for the WT strain ($P < 0.05$). At 72 h, 2,3-BD productivity was 0.64 g/L·h in the recombinant strain and the conversion rate of glucose was 0.47 g/g. For the WT strain, 2,3-BD productivity was 0.31 g/L·h and the conversion rate was 0.39 g/g; these values increased by 106.5% (2,3-BD productivity) and 20.5% (conversion rate of glucose), respectively in the mutant ($P < 0.05$). The lactate and acetate production in the recombinant strain was significantly lower than that in the WT strain (Fig. 2c). The maximum observed acetate production by the WT strain was 4.58 g/L at 144 h, and that in the mutant strain was 1.59 g/L. Thus, the acetate production in the recombinant strain decreased by 62.8% compared with that in the WT strain ($P < 0.05$). The output of ethanol by recombinant strain *K. pneumoniae* HD79-02 was higher than that in the WT strain (maximum 8.11 g/L at 72 h for the mutant strain, 6.36 g/L at 72 h for the parental strain; an increase of 27.5% [$P < 0.05$]).

The typical end products in microaerobic batch fermentations are shown in Table 2 (average values with 95% confidence intervals). Maximum 2,3-BD production by *K. pneumoniae* HD79-02 was increased by 54.9% compared to that by *K. pneumoniae* HD79, and occurred 24 h earlier in *K. pneumoniae* HD79-02. The highest yield of lactate and acetate were reduced by 48.2% and 62.8% respectively in *K. pneumoniae* HD79-02. Simultaneously, the highest ethanol output increased by 27.5% in *K. pneumoniae* HD79-02. Production of other by-products such as succinate and 1,3-PD was similar in the mutant and WT strains.

## Library construction

A cDNA library was obtained from an equal mixture of RNA isolated from the *K. pneumoniae* HD79 and HD79-02 samples, which was used for Illumina 90 bp pair-end sequencing, yielding 14,266,260 reads, 1,283,963,400 bp, and 13,419,787 (94.07%) mapped reads for HD79-02, and 14,202,252 reads, 1,278,202,680 bp, and 13,386,385 (94.26%) mapped reads for HD79. Genome sequences were assembled using Trinity software.

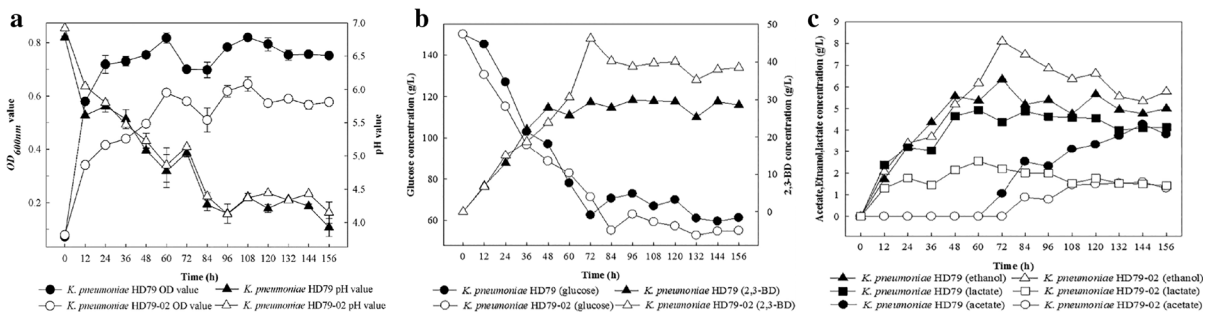


**Fig. 2** Batch fermentation of *K. pneumoniae* HD79 and *K. pneumoniae* HD79-02. **a** black circle, cell growth of *K. pneumoniae* HD79; open circle, cell growth of *K. pneumoniae* HD79-02; black triangle, pH of *K. pneumoniae* HD79 culture; open triangle, pH of *K. pneumoniae* HD79-02 culture. **b** black circle, glucose residue for *K. pneumoniae* HD79; open circle, glucose residue for *K. pneumoniae* HD79-02; black triangle, concentration of 2,3-BD for *K. pneumoniae* HD79; open triangle, concentration of 2,3-BD for *K. pneumoniae* HD79-02. **c** black square, concentration of lactate produced by *K. pneumoniae* HD79; open square, concentration of lactate produced by *K. pneumoniae* HD79-02; black triangle, concentration of ethanol produced by *K. pneumoniae* HD79; open triangle, concentration of ethanol produced by *K. pneumoniae* HD79-02; black circle, concentration of acetate produced by *K. pneumoniae* HD79; open circle, concentration of acetate produced by *K. pneumoniae* HD79-02. The values are the mean of three independent samples

**Table 2** Comparison of batch fermentation of glucose by *K. pneumoniae* HD79 and HD79-02

| Categories | Strain | | Ratio (%) |
|---|---|---|---|
| | HD79 | HD79-02 | |
| 2,3-BD (g/L) | 29.83 ± 0.03 (96 h) | 46.21 ± 0.04 (72 h) | ↑54.9 |
| Lactate (g/L) | 4.94 ± 0.02 (60 h) | 2.56 ± 0.02 (60 h) | ↓48.2 |
| Acetate (g/L) | 4.28 ± 0.02 (144 h) | 1.59 ± 0.03 (144 h) | ↓62.8 |
| Succinate (g/L) | 0.86 ± 0.01 (72 h) | 0.85 ± 0.01 (60 h) | – |
| Ethanol (g/L) | 6.36 ± 0.01 (72 h) | 8.11 ± 0.02 (72 h) | ↑27.5 |
| 1,3-PD (g/L) | 5.33 ± 0.02 (60 h) | 5.62 ± 0.01 (60 h) | – |
| 2,3-BD yield (g/g) | 0.39 ± 0.01 | 0.47 ± 0.01 | ↑20.5 |
| 2,3-BD productivity (g/L·h) | 0.31 ± 0.01 | 0.64 ± 0.01 | ↑106.5 |

Analysis of differentially expressed genes

*Klebsiella pneumoniae* HD79 and HD79-02 samples for sequencing were collected at 6 h of culture. Following comparative analysis with EdgeR, differentially expressed genes in HD79 and HD79-02 revealed obvious differences between the strains. A total of 4628 differentially expressed genes were identified, of which 404 (of 2312) up-regulated genes and 162 (of 2316) down-regulated genes showed statistically significant differences in expression. The differentially expressed genes were analyzed using MA plot (Fig. 3a), and volcano plot (Fig. 3b) was used to show the overall distribution of differential genes and the abundance in the two transcripts. Genes with unknown function or predicted general functions were excluded, and 27 and 24 kinds of functionally annotated genes were identified.

Significant enrichment by pathway allowed the identification of the most important biochemical metabolic pathways and signal transduction pathways in the differentially expressed transcripts (Fig. 3c). The first 20 metabolic pathways of differentially expressed genes were enriched. According to the number of differentially expressed genes in the annotation of metabolic pathway genes, the biosynthesis of amino acids metabolic pathway ranked first, followed by the carbon metabolism pathway, the phosphotransferase system, and pyruvate metabolism.

Annotation of predicted proteins

A sequence similarity search was performed against the non-redundant (Nr), UniProtKB/Swiss-Prot (SwissProt), Gene Ontology (GO), Clusters of Orthologous Groups (COG), and Kyoto Encyclopaedia of Genes and Genomes (KEGG) databases, and GO assignments were used to classify the predicted functions of Sativa mycorrhizal genes. Based on sequence homology, 7839 genes were categorized into 28 functional groups (Fig. 3d). The biological function of these genes included the following molecular processes, intracellular/extracellular enzymes, and structural proteins including hypothetical proteins: phosphofructokinase family protein, pullulanase secretion envelope protein, phosphotransferase system associated protein, propanediol utilization protein, LysR family transcriptional regulator, ethanolamine utilization proteins, ABC transporter permease, translocator protein, LysE family, AraC family transcriptional regulator, major facilitator family transporter, DNA-binding proteins, and other proteins associated with 2,3-BD production. All clusters were then searched against the Cluster of Orthologous Groups (COG) database for functional prediction and classification, which enabled assignment of the eight Nr hits as COG classifications. Among the 28 COG categories, the 'General function prediction' cluster represented the largest group, followed by 'replication, recombination, and repair' and 'transcription', while 'nuclear structure' and 'organelle' were the smallest groups. In each of the three main categories (biological process, cellular component, and molecular function) of the GO classification, metabolic processes, diverse cellular activities, and catalytic activity terms were dominant. Biological processes were related to biological regulation, metabolic regulation, and nuclear transport processes; cell composition, cell membrane composition, and nuclear composition were all functions related to cellular components; and molecular functions were mostly related to nucleic acid transcriptional activators and nuclear transport activities.

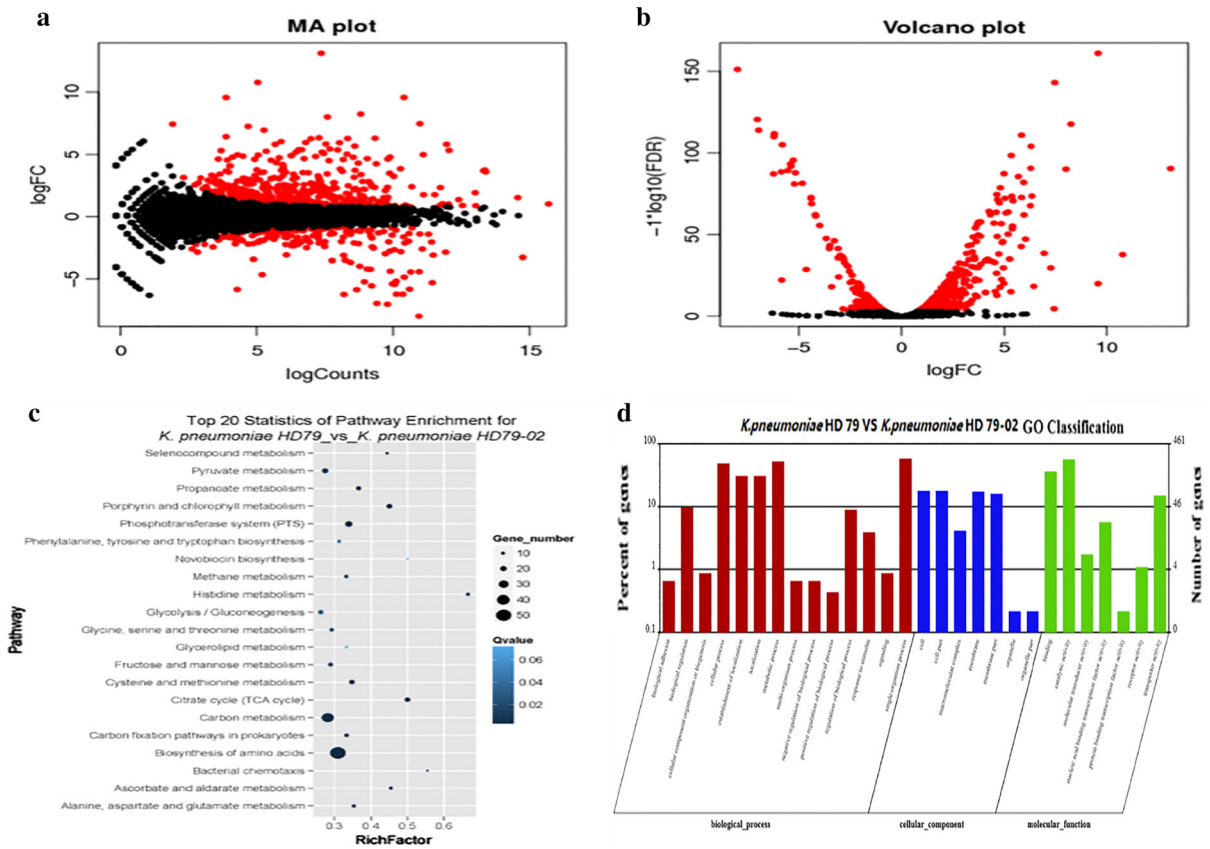


**Fig. 3** MA plot (**a**), Volcano plot (**b**), the top 20 enriched pathways (**c**), and GO classification (**d**) analysis of *K. pneumoniae* HD79 and HD79-02. **a** The Y-axis represents the $\log^2$ times of each differential gene, the X-axis represents the average of the $\log^2$ of the gene. **b** The Y-axis represents the reported error rate, the X-axis represents the $\log^2$ times of each differential gene. Genes that were identified as significantly differentially expressed at a maximum of 0.1% FDR are colored red

## Validation of differentially expressed genes by qRT-PCR

The 2,3-BD-related genes KPK_1166, KPK_2399, KPK_4670, and KPK_2279 were selected for verification by qRT-PCR, and their expression in *K. pneumoniae* HD79-02 was higher than that in HD79, as expected (Fig. 4a). The four genes associated with *Bud*R (KPK_1166, KPK_2399, KPK_4670, KPK_2279) were all clearly up-regulated in HD79-02 compared with the parent strain after 6 h of cell growth, and the amount of acidic by-products were relatively low at this stage. Expression of 2,3-BD biosynthesis-related genes clearly differed between HD79 and HD79-02. Additionally, these genes encoded propanediol and ethanolamine-related proteins that indirectly influenced 2,3-BD production, and were highly expressed in HD79-02.

## Discussion

In this study, we observed different growth conditions in the recombinant and WT strains. The reason for this could be that acetate kinase catalyzes the formation of acetate from acetyl phosphate, accompanied by the formation of adenosine triphosphate (ATP). With the deletion of *ack*, the available energy of the recombinant strain was reduced to some extent, thus affecting the growth rate of the recombinant strain (Förster and Gescher 2014). Another reason could be that the carbon flux of the recombinant strain changed, which affected the distribution and transportation of nutrients

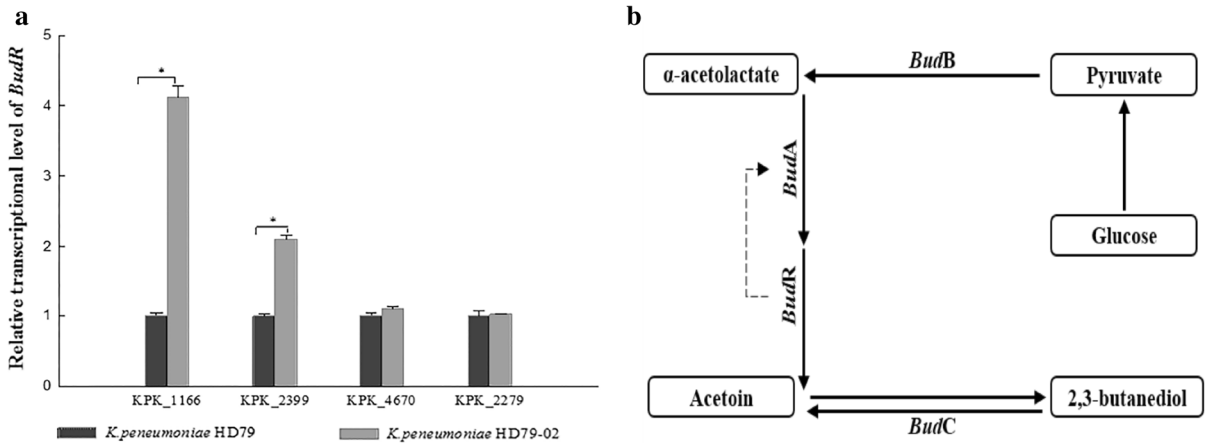


**Fig. 4** Comparison of *Bud*R mRNA levels in *K. pneumoniae* HD79 and HD79-02 (**a**). Function of the *Bud*BAC operon and the *Bud*R gene/*Bud*R regulator in *K. pneumoniae* (**b**).*$P < 0.05$ relative to control

in the recombinant strain, thereby affecting the supply of raw materials necessary for growth and acetate metabolism (You et al. 2008). The culture pH of the recombinant strain was slightly higher than that of the WT strain. This could be because of reduced lactate and acetate production due to disruption of *ldh*A and *ack*, resulting in a slight increase in the pH of the fermentation broth. Further, glucose consumption was increased; this may be due to the consumption of more substrate to maintain cell growth. On the other hand, it could be due to the elimination of by-products, which increased the availability of the carbon source for the 2,3-BD metabolic pathway and thereby increased the yield of 2,3-BD Kim et al. (2013). successfully knocked out the *ldh* of *K. pneumoniae* GSC12206 by λRed homologous recombination and carried out fermentation with glucose as the substrate. The result showed that compared with the WT strain, the lactate production was 92.86% lower than that of the WT strain, while the productivity and yield of 2,3-BD increased by 13% and 60%. Suwannakham et al. (2010) used the λRed homologous recombination technique to knock out *ack* in *P. acidipropionici*, which was used in fermentation with glucose as a substrate. They showed that the yield of propionic acetate increased by 13%, while the yield of acetate decreased by 17%. When *ldh*A and *ald*H were deleted in *K. pneumoniae* 2–1, 1,3-PD production was enhanced and the concentration of by-products was reduced (Chen et al. 2016). In the context of these results, we achieved a good increase in 2,3-BD production. Therefore, the knockout effect was very obvious, and it can better explain the relationship between lactic acid and acetic acid and 2,3-BD production.

Lactate and acetate are typical acidic by-products of *K. pneumoniae* HD79 fermentation to produce 2,3-BD (Guo et al. 2014; Ji et al. 2011) with glucose as a substrate. The production of lactate and acetate consumes energy and inhibits the growth of the host strain. Deletions in recombinant strains are often designed with the intent of maintaining normal physiological metabolic functions; gene knockout therefore often sdoes not cause complete loss of traits or related products, but may considerably reduce their expression. The recombinant strains in this study did not exhibit complete loss of lactate and acetate function; a small amount of lactate and acetate were still produced under conditions of low LDH and ACK activity. This could be because *ldh* had multiple sequences in different genomic regions of *K. pneumoniae* HD79, which belong to the multi-copy functional gene (Markert et al. 1975). Therefore, not all *ldh* was lost, and a small number of genes were still expressed. In addition, lactate may have been produced to balance NADH/$NAD^+$ in the environment. Considering the recombination efficiency factors, it was difficult to screen out multiple cloned knockout clones. After *ack* knock out, the recombinant strain *K. pneumoniae* HD79-02 produces a small amount of acetate by other pathways to maintain normal physiological metabolic function. For example, pyruvate may produce a small amount of acetate via pyruvate oxidase (poxB pathway). A small amount of acetate

could promote the formation of 2,3-BD; maintaining the concentration of acetate at a lower range was therefore a beneficial result (Sang et al. 2017). Succinate is produced by the action of fumarate reductase on fumaric acid. 1,3-PD is produced by the action of 1,3-PD oxidoreductase on 3-hydroxypropionaldehyde. When the genes of certain products are knocked out, there are repercussions in the production of other products. This could be because of changes in the flow of carbon sources (Nguyen et al. 2018).

In this study, all data were above 88%, indicating a high base reading accuracy during sequencing, and sequencing data were adequate to provide functional information. The GC content from the two strains was similar, which confirmed that the sequencing time was sufficient (Kiran Gopinath et al. 2015). Li et al. used transcriptomics to analyze the vulnerable and stable genes in carotid atherosclerotic plaques; 318 genes were up-regulated by and 363 were down-regulated. Volcanic maps were used to identify differential gene expression between the two groups. These were more illustrative of the authenticity and reliability of the results (Li et al. 2018). Guo et al. changed the expression level and genotype of the *rpoD* gene to increase the tolerance of *K. pneumoniae* to xylose and improve the production of 2,3-BD. Differentially expressed genes were mainly involved in signal transduction, membrane transport, carbohydrate metabolism, and energy metabolism (Guo et al. 2018). In summary, by analyzing the differentially expressed genes, it is possible to determine what changes occur in the metabolic pathway in which the gene is involved. A transcriptome analysis of five *K. pneumoniae* strains showed that differences in gene expression mainly occurred in seven aspects including genes coding 2,3-BD biosynthesis (*Bud*A, *Bud*B, *Bud*C), and resulted in metabolism changes (Lee et al. 2015). This is similar to the results of this study wherein 2,3-BD-related genes were differentially expressed and affected the production of 2,3-BD.

The *Klebsiella* species were screened particularly closely by whole-genome sequencing by Macrogen Inc. The amino acid sequence of the putative LysR family transcriptional regulatory protein *Bud*R was obtained. Annealing of this sequence with *K. pneumoniae* MGH 78,578 sequence generated hits based on Cluster of Orthologous Groups (COG) (Heum et al. 2012; Soojin et al. 2013). The 873-nucleotide *Bud*R was located slightly upstream of the *Bud*A (Patel and Jain 2012), and fell into the post translational modification, protein turnover, and chaperones group. In most microorganisms producing 2,3-BD, the key genes (*Bud*B, *Bud*A and *Bud*C) for 2,3-BD production are organized into an operon controlled by the neighboring and divergently transcribed *Bud*R (Ji et al. 2008). In our study, LysR transcriptional regulators were up-regulated in *K. pneumoniae* HD79-02, suggesting that regulation of *Bud*R expression is important in 2,3-BD biosynthesis. However, the *ldh* and *ack* genes encoding proteins involved in the biosynthesis of acidic by-products were down-regulated during the log and stationary phases in HD79-02. Thus, biosynthesis of 2,3-BD likely played a role in diverting pyruvate flux away from the production of acidic substrates such as lactate, formate, and acetate to prevent the culture medium form becoming too acidic for cell growth (Sun et al. 2009; Wang et al. 2019). While these proteins were not directly involved in production of 2,3-BD, they likely shifted the carbon flux towards the biosynthesis of alcohols. The transcriptional regulator *Bud*R regulated the expression of *Bud*A, *Bud*B, *Bud*C, which directly affected the viability of key enzymes producing 2,3-BD, and therefore increased production of 2,3-BD (Fig. 4b). *ldh* and *ack* can directly regulate the production of lactic acid and acetic acid. The production of 2,3-BD can be greatly increased by reducing acetic acid and lactic acid. BudR is related to three key genes, *Bud*A, *Bud*B, and *Bud*C, which produce 2,3-BD. As a transcriptional activator to increase 2,3-BD production. In addition, these genes encode propylene glycol and ethanolamine-related proteins, which indirectly affect 2,3-BD production, and they are highly expressed in *K. pneumoniae* HD79-02 for increasing 2,3-BD production. The lower concentration of acetic acid can promote 2,3-BD production, and the transcriptional activator BudR can also induce the formation of 2,3-BD under acidic conditions. In other studies, we have confirmed acetic acid can indeed promote the expression of *Bud*A and *Bud*B genes at a certain concentration. Therefore, acetic acid may act on the *Bud*R gene, which may increase 2,3-BD production. The biosynthetic pathway of 2,3-BD therefore seems to be regulated by three main factors: the inducers (lactate and acetate), regulator (*Bud*R), and carbon flux. Although the changes in 2,3-BD, lactate, and acetate levels reported in this work were relatively moderate, our results could significantly

reduce the production cost of 2,3-BD. Our results greatly improve our understanding of the mechanism of 2,3-BD production and the interaction between acids and alcohols, and provide a sound theoretical basis for further improvement of 2,3-BD production.

**Acknowledgement** This work was supported by the National Natural Science Foundation of China (Grant Nos 31570492, 31770544) and Heilongjiang Provincial Key Laboratory of Plant Genetic Engineering and Biological Fermentation Engineering for Cold Region.

**Compliance with ethical standards**

**Conflict of interest** The authors declare that there are no conflicts of interest.

## References

Białkowska AM (2016) Strategies for efficient and economical 2,3-butanediol production: new trends in this field. World J Microbiol Biotechnol 32:1–14

Chen L, Ma C, Wang R, Yang J, Zheng H (2016) Deletion of *ldh*A and *ald*H genes in *Klebsiella pneumoniae* to enhance 1,3-propanediol production. Biotechnol Lett 38:1769–1774

Dimont E, Shi J, Kirchner R, Hide W (2015) edgeRun: an R package for sensitive, functionally relevant differential expression discovery using an unconditional exact test. Bioinform 31:2589–2590

Förster AH, Gescher J (2014) Metabolic engineering of *Escherichia coli* for production of mixed-acid fermentation end products. Biotechnol Bioeng 2:16

Gao Y, Huang H, Chen S, Qi G (2018) Production of optically pure 2,3-butanediol from *Miscanthus floridulus* hydrolysate using engineered *Bacillus licheniformis* strains. World J Microbiol Biotechnol 34:66

Ge Y, Li K, Li L, Chao G, Zhang L, Ma C, Ping X (2016) Contracted but effective: production of enantiopure 2,3-butanediol by thermophilic and GRAS *Bacillus licheniformis*. Green Chem 18:4693–4703

Guo X, Cao C, Wang Y, Li C, Wu M, Chen Y, Zhang C, Pei H, Xiao D (2014) Effect of the inactivation of lactate dehydrogenase, ethanol dehydrogenase, and phosphotransacetylase on 2,3-butanediol production in *Klebsiella pneumoniae* strain. Biotechnol Biofuels 7:44

Guo XW, Zhang Y, Li LL, Guan XY, Guo J, Wu DG, Chen YF, Xiao GD (2018) Improved xylose tolerance and 2,3-butanediol production of *Klebsiella pneumoniae* by directed evolution of rpoD and the mechanisms revealed by transcriptomics. Biotechnol Biofuels 11:307

Harney E, Dubief B, Boudry P, Basuyaux O, Schilhabel MB, Huchette S, Paillard C, Nunes FLD (2016) De novo assembly and annotation of the European abalone *Haliotis tuberculata* transcriptome. Mar Genom 28:11–16

Harvianto GR, Haider J, Hong J, Long NVD, Shim JJ, Cho MH, Kim WK, Lee M (2018) Purification of 2,3-butanediol from fermentation broth: process development and techno-economic analysis. Biotechnol Biofuels 11:18

Heum SS, Sewhan K, Jae Young K, Soojin L, Youngsoon U, Min-Kyu O, Young-Rok K, Jinwon L (2012) Complete genome sequence of the 2,3-butanediol-producing *Klebsiella pneumoniae* strain KCTC 2242. J Bacteriol 194:2736–2737

Ishii J, Morita K, Ida K, Kato H, Kinoshita S, Hataya S, Shimizu H, Kondo A, Matsuda F (2018) A pyruvate carbon flux tugging strategy for increasing 2,3-butanediol production and reducing ethanol subgeneration in the yeast *Saccharomyces cerevisiae*. Biotechnol Biofuels 11:180

Ji XJ, Huang H, Li S, Du J, Lian M (2008) Enhanced 2,3-butanediol production by altering the mixed acid fermentation pathway in *Klebsiella oxytoca*. Biotechnol Lett 30:731–734

Ji XJ, Huang H, Ouyang PK (2011) Microbial 2,3-butanediol production: a state-of-the-art review. Biotechnol Adv 29:351–364

Kanehisa M, Furumichi M, Mao T, Sato Y, Morishima K (2017) KEGG: new perspectives on genomes, pathways, diseases and drugs. Nucleic Acids Res 45:D353–D361

Kim DK, Rathnasingh C, Song H, Lee HJ, Seung D, Yong KC (2013) Metabolic engineering of a novel *Klebsiella oxytoca* strain for enhanced 2,3-butanediol production. J Biosci Bioeng 116:186–192

Kiran Gopinath B, Vivek Nagaraj T, Rohit Nandan S, Madavan V (2015) Ameliorated de novo transcriptome assembly using illumina paired end sequence data with trinity assembler. Genomics 5:352–359

Lee S, Kim B, Jeong D, Oh M, Um Y, Kim YR, Kim J, Lee J (2013) Observation of 2,3-butanediol biosynthesis in Lys regulator mutated *Klebsiella pneumoniae* at gene transcription level. J Biotechnol 168:520–526

Lee S, Kim B, Yang J, Jeong D, Park S, Sang HS, Kook JH, Yang KS, Lee J (2015) Comparative whole genome transcriptome and metabolome analyses of five *Klebsiella pneumonia* strains. Bioprocess Biosyst Eng 38:2201–2219

Li T, Zhang X, Zhang J, Liu R, Gu C (2018) The transcriptome difference between vulnerable and stable carotid atherosclerotic plaque. Int J Clin Exp Med 11:8988–9004

Markert CL, Shaklee JB, Whitt GS (1975) Evolution of a gene. multiple genes for LDH isozymes provide a model of the evolution of gene structure, function and regulation. Science 189:102–114

Mayer D, Schlensog V, Ck AB (1995) Identification of the transcriptional activator controlling the butanediol fermentation pathway in *Klebsiella terrigena*. J Bacteriol 177:5261–5269

Nguyen AD, Hwang IY, Lee OK, Kim D, Kalyuzhnaya MG, Mariyana R, Hadiyati S, Kim MS, Lee EY (2018) Systematic metabolic engineering of *Methylomicrobium alcaliphilum* 20Z for 2,3-butanediol production from methane. Metab Eng 47:323–333

Park JM, Rathnasingh C, Song H (2015) Enhanced production of (R, R)-2,3-butanediol by metabolically engineered *Klebsiella oxytoca*. J Ind Microbiol Biotechnol 42:1419–1425

Park SW, Lee YJ, Lee WJ, Jee Y, Choi WY (2016) One-step reverse transcription-polymerase chain reaction for ebola and marburg viruses. Int J Env Res Pub Health 7:205–209

Patel RK, Jain M (2012) NGS QC Toolkit: a toolkit for quality control of next generation sequencing data. PLoS ONE 7:e30619

Petrov K, Petrova P (2009) High production of 2,3-butanediol from glycerol by *Klebsiella pneumoniae* G31. Appl Microbiol Biotechnol 84:659–665

Rathnasingh C, Park JM, Kim DK, Song H, Yong KC (2016) Metabolic engineering of *Klebsiella pneumoniae* and in silico investigation for enhanced 2,3-butanediol production. Biotechnol Lett 38:975–982

Sang JL, Han SC, Chan KK, Thapa LP, Park C, Kim SW (2017) Process strategy for 2,3-butanediol production in fed-batch culture by acetate addition. J Ind Eng Chem 56:157–162

Sikora B, Kubik C, Kalinowska H, Gromek E, Białkowska A, Jędrzejczak-Krzepkowska M, Schüett F, Turkiewicz M (2015) Application of byproducts from food processing for production of 2,3-butanediol using *Bacillus amyloliquefaciens* TUL 308. Prep Biochem Biotech 46:610–619

Sun LH, Wang XD, Dai JY, Xiu ZL (2009) Microbial production of 2,3-butanediol from Jerusalem artichoke tubers by *Klebsiella pneumoniae*. Appl Microbiol Biot 82:847–852

Suwannakham S, Huang Y, Yang ST (2010) Construction and characterization of ack knock-out mutants of *Propionibacterium acidipropionici* for enhanced propionic acid fermentation. Biotechnol Bioeng 94:383–395

Taeyeon K, Sukhyeong C, Sun-Mi L, Min WH, Jinwon L, Youngsoon U, Jin-Ho S (2016) High production of 2,3-Butanediol (2,3-BD) by *Raoultella ornithinolytica* B6 via optimizing fermentation conditions and overexpressing 2,3-BD synthesis genes. PLoS ONE 11:0165076

Theissinger K, Falckenhayn C, Blande D, Toljamo A, Gutekunst J, Makkonen J, Jussila J, Lyko F, Schrimpf A, Schulz R, Kokko H (2016) De novo assembly and annotation of the freshwater crayfish *Astacus astacus* transcriptome. Mar Genomics 28:7–10

Wang P, Zhang J, Feng J, Wang S, Guo L, Wang Y, Lee YY, Taylor S, McDonald T, Wang Y (2019) Enhancement of acid re-assimilation and biosolvent production in *Clostridium saccharoperbutylacetonicum* through metabolic engineering for efficient biofuel production from lignocellulosic biomass. Bioresource Technol 281:217–225

Yang Z, Zhang Z (2018) Production of (2R, 3R)-2,3-butanediol using engineered *Pichia pastoris*: strain construction, characterization and fermentation. Biotechnol Biofuels 11:35

Yang T, Rao Z, Zhang X, Xu M, Xu Z, Yang ST (2017) Metabolic engineering strategies for acetoin and 2,3-butanediol production: advances and prospects. Crit Rev Biotechnol 37:1–16

You KO, Park SH, Seol EH, Kim SH, Mi SK, Hwang JW, Dewey DY (2008) Carbon and energy balances of glucose fermentation with hydrogen-producing bacterium *Citrobacter amalonaticus* Y19. J Microbiol Biotechnol 18:532–538